Violation of the Bell–Clauser-Horne-Shimony-Holt inequality using imperfect photodetectors with optical hybrid states

Hyukjoon Kwon and Hyunseok Jeong[*]

Center for Macroscopic Quantum Control, Department of Physics and Astronomy, Seoul National University, Seoul 151-742, Korea

We show that a Bell inequality test using an optical hybrid state between a polarized single photon and a coherent field can be highly robust against detection inefficiency. The Bell violation occurs until the efficiency becomes as low as 67% even though its degree becomes small as the detection efficiency degrades. We consider on/off and photon number parity measurements, respectively, for the Bell test and they result in similar conditions. If the detection efficiency is higher than 98.68%, parity measurements give larger Bell violations close to Cirel'son's bound, while on/off measurements give larger but moderate violations for realistic values of detector efficiency. Experimental realization of our proposal seems feasible in the near future for the implementation of a loophole-free Bell inequality test.

I. INTRODUCTION

The argument by Einstein, Podolsky, and Rosen (EPR) provoked debates on the incompatibility between quantum mechanics and local realism [1]. Around 30 years after the work of EPR was published, Bell in his celebrated paper suggested an inequality that enables one to test quantum mechanics against local realism [2]. Since then, various versions of Bell's inequality have been suggested including that of Clauser, Horne, Shimony, and Holt (CHSH), known as the Bell-CHSH inequality [3]. The Bell-CHSH inequality has been theoretically studied within the frameworks of N-dimensional systems [4–6] and continuous variables in phase space [7–12].

Meanwhile, various experimental efforts have been made to observe violation of Bell's inequality, yet no experiment has been found to be completely loophole-free. In general, experiments using atoms [13,14] have suffered from the locality loophole [15,16], while optical experiments [17–20] have not been free from the detection (or fair-sampling) loophole [21]. In order to close the detection loophole for the Bell-CHSH inequality test, 82.8% of detector efficiency is required when using a maximally entangled bipartite system. It was shown that Bell-type inequality with nonmaximally entangled states could lower the threshold efficiency to 66.7% [22]. The experimental observation of Bell inequality violation using partially entangled photons without the fair-sampling assumption was reported recently [23].

In order to lower the detection efficiency threshold for a loophole-free Bell test, schemes based on high dimensional [24–28], multiphoton [29,30], and multimode [31] states have been suggested. A study on an asymmetric Bell-type inequality, assuming perfect detection on one side, shows that 43% of detection efficiency is required [27], while a scheme using qudit systems requires 61.8% of threshold efficiency [28]. In principle, macroscopic entanglement enables one to perform a Bell inequality test free from the detection inefficiency [30]. Continuous variable systems with homodyne detection have also been investigated to close the detection loophole [32–35]. Atom-fields entanglement to combine the advantages of both

the atomic and optical systems have been studied in the context of loophole-free Bell inequality tests [31,34,36–41] and several related experiments have been reported [42–44]. It was shown that a hybrid detection scheme, combining homodyne detection and photodetection, with atom-photon entanglement may be used for loophole-free Bell tests under moderate transmission losses and detection efficiencies [40,41].

In this paper, we study optical hybrid entanglement between a polarized single photon and a coherent-state field for Bell inequality tests using inefficient detectors. We employ two different kinds of measurements for the coherent-state field, photon on/off measurement and photon number parity measurement, to investigate the Bell-CHSH inequality. We find that the Bell-CHSH inequality is violated for low coherent amplitudes ($|\alpha| < 1.0$) with detection efficiency higher than 67%. When realistic detection efficiency is assumed (i.e., smaller than 98.68%), the scheme based on on/off measurements gives larger Bell violation than the one based on photon number parity measurements, while nearly perfect detector efficiency provides higher Bell values close to Cirel'son's bound $2\sqrt{2}$ for the parity measurement scheme. However, threshold values for detection efficiencies over which Bell violations occur are similar for both the measurement schemes.

II. BELL-CHSH INEQUALITY TEST WITH OPTICAL HYBRID STATES

In this paper, we are interested in an optical hybrid state with entanglement between a polarized single photon and a coherent state,

$$|\Psi\rangle = \frac{1}{\sqrt{2}}(|H\rangle_A|\alpha\rangle_B + |V\rangle_A|-\alpha\rangle_B), \qquad (1)$$

where $|H\rangle$ and $|V\rangle$ refer to the horizontal and vertical polarization states of a photon each, and $|\pm\alpha\rangle$ are coherent states of amplitudes $\pm\alpha$. Such hybrid entangled states are particularly useful for deterministic quantum teleportation and resource-efficient quantum computing using linear optics [45] as well as for information transfer between different types of qubits [46]. It was shown that this type of entanglement can be obtained if a weak cross-Kerr nonlinear interaction is

---

*h.jeong37@gmail.com

available [47]. It is highly challenging to implement cross-Kerr nonlinearity with high fidelity [48,49], while there have been several proposals to obtain such high-fidelity cross-Kerr interactions [50–52].

A. Bell-CHSH inequality using on/off and parity measurements

In order to perform Bell inequality tests, an entangled state should be shared by two locally separate parties. With regard to the state in Eq. (1), the single-photon part with the polarization degree of freedom and the coherent-state part with amplitudes $\pm\alpha$ are subscripted by A and B, respectively. Each party may locally perform unitary operations and dichotomic measurements. In order to construct a Bell-CHSH inequality, each measurement outcome is determined as either $+1$ or -1. We may choose $\hat{\Pi}_A = |H\rangle\langle H| - |V\rangle\langle V|$ for polarization measurements for the single-photon part and

$$\hat{\Pi}_B = \begin{cases} |0\rangle\langle 0| - \sum_{n=1}^{\infty} |n\rangle\langle n| & \text{(on/off)} \\ \sum_{n=0}^{\infty} (|2n\rangle\langle 2n| - |2n+1\rangle\langle 2n+1|) & \text{(parity)} \end{cases}$$
(2)

for on/off and photon number parity measurements each. Outcomes ± 1 denote no-click/click events for on/off measurements and even/odd number results for photon number parity measurements. An arbitrary unitary operation on a single-photon qubit with the qubit basis of $|H\rangle$ and $|V\rangle$ can be represented by

$$U(\xi) = \begin{pmatrix} \cos|\xi| & \frac{\xi}{|\xi|}\sin|\xi| \\ -\frac{\xi^*}{|\xi|}\sin|\xi| & \cos|\xi| \end{pmatrix}$$
(3)

with complex variable ξ. The displacement operation $D(\beta) = e^{\beta\hat{a}^\dagger - \beta^*\hat{a}}$ is used as a unitary operation on the coherent-state part (i.e., mode B), where β is a complex variable. A previous result shows that the displacement operator approximately acts as a qubit rotation for a coherent-state qubit with basis $|\pm\alpha\rangle$ [12]. The expectation value of the joint measurement is obtained as

$$E(\xi,\beta) = \langle \hat{O}_A \otimes \hat{O}_B \rangle,$$
(4)

where $\hat{O}_A(\xi) = U(\xi)\hat{\Pi}_A U^\dagger(\xi)$ and $\hat{O}_B(\beta) = D(\beta)\hat{\Pi}_B D^\dagger(\beta)$. The Bell-CHSH inequality is then defined as $|B(\xi_1,\xi_2,\beta_1,\beta_2)| \leqslant 2$ with the Bell function

$$B(\xi_1,\xi_2,\beta_1,\beta_2) = E(\xi_1,\beta_1) + E(\xi_1,\beta_2) \\ + E(\xi_2,\beta_2) - E(\xi_2,\beta_1).$$
(5)

We define $\xi = -(\theta/2)e^{-i\phi}$ and $\beta = |\beta|e^{i\Phi}$ with $0 \leqslant \theta < \pi$, $0 \leqslant \phi$, and $\Phi < 2\pi$ for simplicity. Without loss of generality, we take α to be real because the phase of α may be absorbed by Φ. We obtain the expectation values as

$$E^{\text{on/off}}(\theta,\phi,|\beta|,\Phi)$$
$$= 2\cos\theta\, e^{-(|\alpha|^2+|\beta|^2)}\sinh(2|\alpha||\beta|\cos\Phi)$$
$$+ 2\sin\theta\, e^{-(|\alpha|^2+|\beta|^2)}\cos(2|\alpha||\beta|\sin\Phi - \phi)$$
$$- \sin\theta\, e^{-2|\alpha|^2}\cos\phi,$$
(6)

$$E^{\text{parity}}(\theta,\phi,|\beta|,\Phi) = \cos\theta\, e^{-2(|\alpha|^2+|\beta|^2)}\sinh(4|\alpha||\beta|\cos\Phi)$$
$$+ \sin\theta\, e^{-2|\beta|^2}\cos(4|\alpha||\beta|\sin\Phi - \phi)$$
(7)

by applying on/off and photon number parity measurements, respectively, on the coherent-state part.

B. Photodetector efficiency and the detection loophole

A physical model of an imperfect photodetector with detection efficiency p is described by a beam splitter of transmission coefficient $\sqrt{p}$ before a perfect photodetector. In terms of positive operator-valued measurement with the photon number basis, a photodetector with efficiency p may be written as [53]

$$\hat{E}_p^{(n)} = \sum_{m=0}^{\infty} \binom{n+m}{n} p^n(1-p)^m |n+m\rangle\langle n+m|.$$
(8)

Then the effective on/off measurement of detection efficiency η_B becomes

$$\hat{\Pi}_{B,\text{eff}}^{\text{on/off}} = \hat{E}_{\eta_B}^{(0)} - \sum_{n=1}^{\infty} \hat{E}_{\eta_B}^{(n)} = \sum_{m=0}^{\infty} [2(1-\eta_B)^m |m\rangle\langle m| - \sum_{n=0}^{\infty} \binom{n+m}{n} \eta_B^n(1-\eta_B)^m |n+m\rangle\langle n+m|].$$
(9)

Similarly, the effective photon number parity measurement is given by

$$\hat{\Pi}_{B,\text{eff}}^{\text{parity}} = \hat{E}_{\eta_B}^{\text{(even)}} - \hat{E}_{\eta_B}^{\text{(odd)}} = \sum_{m=0}^{\infty} \sum_{n=0}^{\infty} \left[\binom{2n+m}{2n} \eta_B^{2n}(1-\eta_B)^m |2n+m\rangle\langle 2n+m| \right.$$

$$\left. - \binom{2n+1+m}{2n+1} \eta_B^{2n+1}(1-\eta_B)^m |2n+1+m\rangle\langle 2n+1+m| \right].$$
(10)

In order to avoid the detection loophole, we assign $+1$ for a "no-detection" outcome on the polarization part. Provided the polarization measurement detection efficiency is η_A, the expectation value for the combined measurement is given by

$$E_{\text{eff}} = \eta_A \langle \hat{O}_A \otimes \hat{O}_{B,\text{eff}} \rangle + (1-\eta_A) \text{Tr}_B[\hat{O}_{B,\text{eff}} \rho_B],$$
(11)

where ρ_B is a reduced density matrix obtained by tracing over polarization part A, i.e.,

$$\rho_B = \text{Tr}_A(\rho) = \frac{1}{2}(|\alpha\rangle\langle\alpha| + |-\alpha\rangle\langle-\alpha|).$$
(12)

Each term in Eq. (10) could be directly calculated as

$$\langle \hat{O}_A \otimes \hat{O}_{B,\text{eff}}^{\text{on/off}} \rangle$$
$$= 2 \cos \theta e^{-\eta_B(|\alpha|^2+|\beta|^2)} \sinh(2\eta_B|\alpha||\beta| \cos \Phi)$$
$$+ 2 \sin \theta e^{-(2-\eta_B)|\alpha|^2-\eta_B|\beta|^2} \cos(2\eta_B|\alpha||\beta| \sin \Phi - \phi)$$
$$- \sin \theta e^{-2|\alpha|^2} \cos \phi, \tag{13}$$

$$\text{Tr}_B\big[\hat{O}_{B,\text{eff}}^{\text{on/off}} \rho_B\big] = 2e^{-\eta_B(|\alpha|^2+|\beta|^2)} \cosh(2\eta_B|\alpha||\beta| \cos \Phi) - 1 \tag{14}$$

for photon on/off measurements and

$$\langle \hat{O}_A \hat{O}_{B,\text{eff}}^{\text{parity}} \rangle = \cos \theta e^{-2\eta_B(|\alpha|^2+|\beta|^2)} \sinh(4\eta_B|\alpha||\beta| \cos \Phi)$$
$$+ \sin \theta e^{-2(1-\eta_B)|\alpha|^2-2\eta_B|\beta|^2}$$
$$\times \cos(4\eta_B|\alpha||\beta| \sin \Phi - \phi), \tag{15}$$

$$\text{Tr}_B\big[\hat{O}_{B,\text{eff}}^{\text{parity}} \rho_B\big] = e^{-2\eta_B(|\alpha|^2+|\beta|^2)} \cosh(4\eta_B|\alpha||\beta| \cos \Phi) \tag{16}$$

for photon number parity measurements.

III. OPTIMIZATION

In order to observe violation of the Bell-CHSH inequality, it is important to find optimizing conditions for local unitary variables under which the Bell functions have largest values. The optimizing conditions presented throughout this paper are numerically found [54], and wherever possible, we try to find corresponding analytical expressions.

A. Perfect photodetector efficiency

We first suppose perfect efficiencies for all detectors used for Bell inequality tests. In the case of photon on/off measurements, optimizing conditions can be obtained as [39]

$$\xi_1 = -\frac{\pi}{4}, \qquad \xi_2 = 0, \qquad \beta_1 = -\beta_2 = -|\beta| \tag{17}$$

with $|\beta|$ satisfying

$$|\beta| \left[1 + \sinh (2|\alpha||\beta|)\right] = |\alpha| \cosh (2|\alpha||\beta|). \tag{18}$$

We plot the Bell function in Fig. 1 and note that as the coherent amplitude $|\alpha|$ increases the maximized Bell value increases up to $|B|_{\text{max}}^{\text{on/off}} \approx 2.61$ for $|\alpha| \approx 0.664$. However, Fig. 1 also shows that further increase of $|\alpha|$ results in lower maximized Bell values. This can be attributed to the fact that the probability of "no-click" on a photodetector becomes lower when $|\alpha|$ becomes larger [12].

We also find the optimizing conditions for photon number parity measurements as

$$\xi_1 = -\frac{\pi}{4}, \quad \xi_2 = i\frac{\pi}{4}, \quad \beta_1 = -\beta_2 = -i|\beta| \tag{19}$$

with $|\beta|$ satisfying $\tan [4|\alpha||\beta|] = (|\alpha| - |\beta|)/(|\alpha| + |\beta|)$ nearest to zero. One may expect that the Bell value would increase as $|\alpha|$ increases because probabilities to have even and odd photon numbers in a coherent state become equal as $|\alpha| \to \infty$. In practice, we note that Bell value of parity measurements rapidly approaches Cirel'son's bound $2\sqrt{2}$ when $|\alpha| \gg 1$.
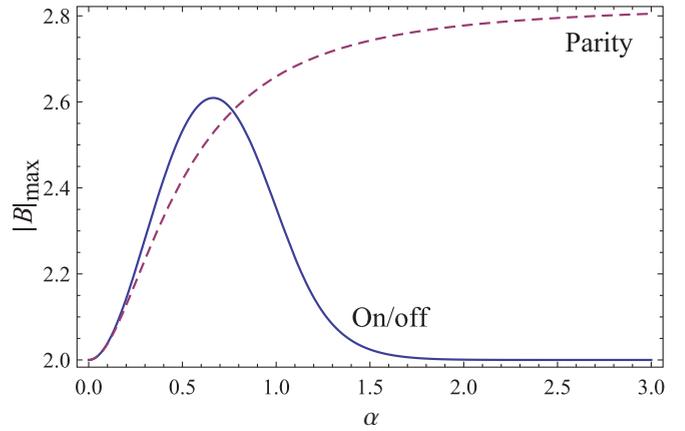
FIG. 1. (Color online) Maximized Bell value $|B|_{\text{max}}$ for varying α with perfect detector efficiency. The solid curve refers to photon on/off measurements, while the dashed curve refers to photon number parity measurements.

B. Imperfect detection for coherent-state fields

Now we consider the situation of perfect polarization measurements ($\eta_A = 1$) and imperfect coherent field measurements ($\eta_B \neq 1$). Optimizing conditions for photon on/off measurements can be obtained by $\xi_1 = -\pi/4$, $\xi_2 = 0$, and $\beta_1 = -\beta_2 = -|\beta|$ to be real with $|\beta|$ satisfying

$$|\beta| e^{-2(1-\eta_B)|\alpha|^2} + |\beta| \sinh(2\eta_B|\alpha||\beta|)$$
$$- |\alpha| \cosh(2\eta_B|\alpha||\beta|) = 0. \tag{20}$$

In this case, the Bell value becomes

$$B^{\text{on/off}}(\xi_1,\xi_2,\beta_1,\beta_2)$$
$$= 4e^{-\eta_B(|\alpha|^2+|\beta|^2)}[e^{-(1-\eta_B)|\alpha|^2}$$
$$+ \sinh(2\eta_B|\alpha||\beta|)] - 2e^{-2|\alpha|^2}. \tag{21}$$

Figure 2 shows that the maximum Bell value is obtained for $0.66 < |\alpha| < 0.71$ and the optimizing coherent amplitude
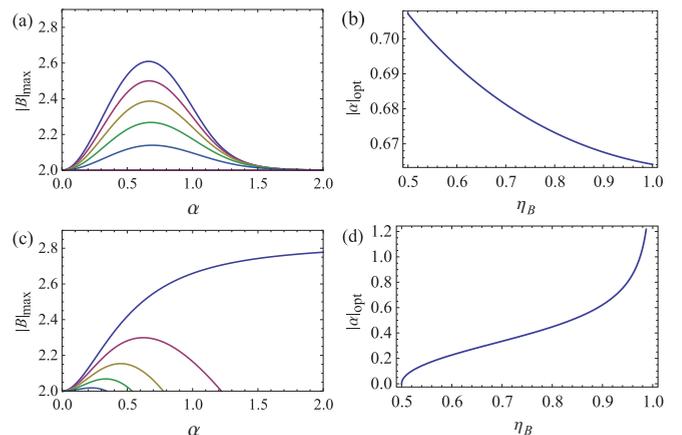
FIG. 2. (Color online) (a) Maximized Bell value for on/off measurements $|B|_{\text{max}}^{\text{on/off}}$ and (b) optimizing $|\alpha|_{\text{opt}}$ for each coherent measurement detection efficiency. (c) Maximized Bell value for parity measurements $|B|_{\text{max}}^{\text{parity}}$ and (d) optimizing $|\alpha|_{\text{opt}}$. In both the cases, the detection efficiency η_B for the coherent-state part decreases by 0.1 from the perfect value ($\eta_B = 1$) to $\eta_B = 0.5$.
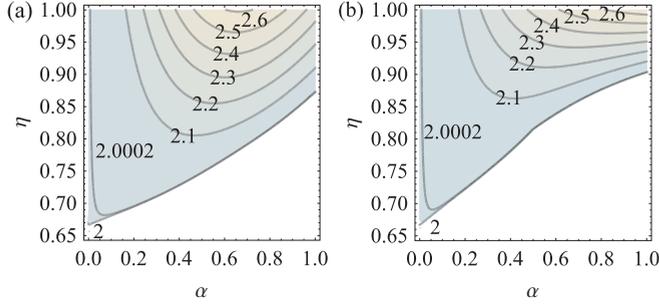
FIG. 3. (Color online) Maximized Bell-CHSH functions in terms of detection efficiency η for both modes and coherent amplitude α for (a) on/off and (b) parity measurement schemes. The detection efficiency threshold to violate the Bell-CHSH inequality is about 67% when the coherent amplitude is low.

$|\alpha_{\text{opt}}|$ monotonically decreases as the detector efficiency increases. Violation of the Bell-CHSH inequality occurs until the detection efficiency reaches 0.5. This result is consistent with the equivalent Bell inequality test using entanglement between an atom and a coherent state in a cavity [39].

We find that optimizing conditions for photon number parity measurements are $\xi_1 = -\pi/4$, $\xi_2 = i\pi/4$, and $\beta_1 = -\beta_2 = -i|\beta|$ to be pure imaginary. Here, $|\beta|$ is the solution of

$$\tan(4\eta_B|\alpha||\beta|) = \frac{|\alpha| - |\beta|}{|\alpha| + |\beta|} \quad (22)$$

nearest to zero, and the Bell function is

$$
\begin{aligned}
B^{\text{parity}}&(\xi_1, \xi_2, \beta_1, \beta_2) \\
&= 2e^{-2(1-\eta_B)|\alpha|^2 - 2\eta_B|\beta|^2}[\cos(4\eta_B|\alpha||\beta|) + \sin(4\eta_B|\alpha||\beta|)].
\end{aligned}
\quad (23)
$$

The optimizing coherent amplitude $|\alpha_{\text{opt}}|$ increases when the detection efficiency becomes larger. This is opposite to the case of an on/off measurement scheme, due to the fact when the efficiency of the photon number parity measurement is low, $|\alpha|$ should be small to reduce the possibility of parity flips. In most of the imperfect detector efficiency conditions, the on/off measurement scheme gives higher violation of the Bell-CHSH inequality than the parity measurement scheme. However, the values of the detection efficiency required to violate the Bell-CHSH inequality are the same (50%) for both schemes.
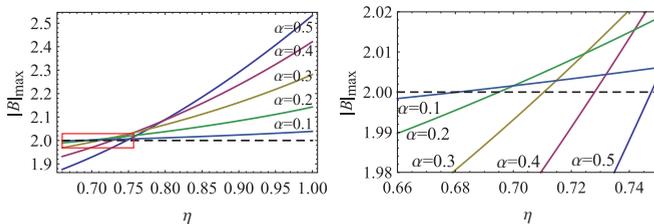
FIG. 4. (Color online) Maximum Bell value via detector efficiency with varying coherent amplitude from 0.1 to 0.5 for the on/off measurement scheme. The right-hand-side figure represents the boxed region of the left-hand-side one.
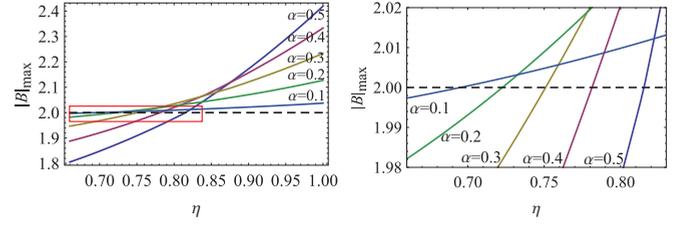
FIG. 5. (Color online) Maximum Bell values against detection efficiency with varying coherent amplitudes from 0.1 to 0.5 for the parity measurement scheme. The right-hand-side figure represents the boxed region of the left-hand-side one.

C. Imperfect detectors for both measurements

We now consider the most realistic case in which both the polarization measurement and the coherent field measurement are imperfect ($\eta_A < 1$ and $\eta_B < 1$). In this case, a nontrivial calculation is needed to obtain the optimizing conditions. It is still sufficient to take real ξ and β for optimizing conditions of photon on/off measurements, but with $|\beta_1| \neq |\beta_2|$. On the other hand, the optimizing parameters for photon number parity measurements tend to have different conditions by detection efficiency of photodetector. When the detection efficiency is high, we find $|\xi_1| = |\xi_2| = \pi/4$ and β_1, β_2 to be pure imaginary for the optimization. If the detector efficiency is low, the optimizing conditions could be chosen to be the same with those of the on/off measurement scheme (see the Appendix).

We first assume the same detection efficiency $\eta_A = \eta_B = \eta$ on the polarization and the coherent field measurements. Figure 3 shows that the degree of Bell violation and the optimizing coherent amplitudes for both the measurement schemes decrease when the detector efficiency η decreases. For example, with $\eta = 0.8$, on/off measurements give the maximum Bell violation of $|B|^{\text{on/off}}_{\text{max}} \approx 2.091$ at $|\alpha| \approx 0.458$, while parity measurements give $|B|^{\text{parity}}_{\text{max}} \approx 2.035$ at $|\alpha| \approx 0.293$. If detector efficiency becomes $\eta = 0.7$, the maximum Bell value and the optimizing coherent amplitude decrease to $|B|^{\text{on/off}}_{\text{max}} \approx 2.0022$ ($|\alpha| \approx 0.155$) and $|B|^{\text{parity}}_{\text{max}} \approx 2.0006$ ($|\alpha| \approx 0.078$) for each measurement scheme. Figures 4 and 5 reveal that there is a trade-off between the degree of Bell violation and the detector efficiency threshold by using different coherent amplitudes $|\alpha|$. Employing a low coherent amplitude demands low detection efficiency in order to see Bell inequality violation but the degree of the violation would be small. Also we note from Fig. 6(a) that with symmetric detector efficiency
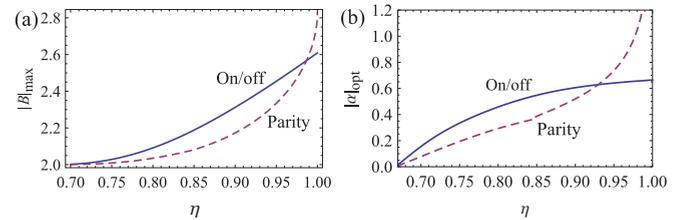
FIG. 6. (Color online) (a) Comparison of Bell violation $|B|_{\text{max}}$ and (b) optimizing coherent amplitude $|\alpha|_{\text{opt}}$ between on/off (solid line) and parity (dashed line) measurements assuming symmetric detector efficiency η. On/off measurements give higher Bell value than parity measurements for $\eta < 0.9868$.
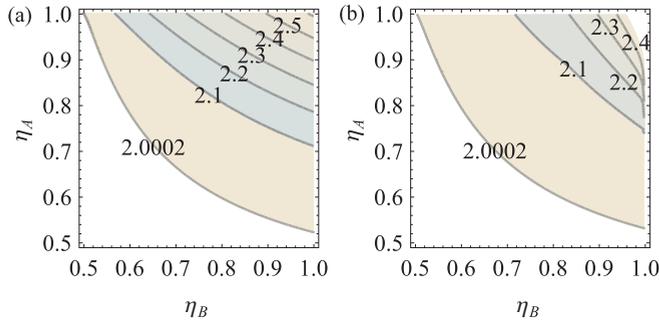
FIG. 7. (Color online) Maximized Bell-CHSH value as a function of detection efficiencies for (a) on/off and (b) parity measurement schemes. Axis labels η_A and η_B refer to polarization (single photon) and coherent field measurement efficiencies, respectively. The optimizing coherent amplitudes were taken for each detection efficiency.

η lower than 98.68%, on/off measurements provide higher Bell violation than parity measurements.

We numerically find that the Bell-CHSH inequality violation occurs until the detection efficiency reaches 67% for both measurement schemes as presented in Fig. 3. This value of the detection efficiency is lower than 82.8% obtained by employing maximally entangled states and similar to the threshold efficiency for the Bell's inequality test using non-maximally entangled states [22]. We note that the maximum Bell violation occurs at $|\alpha| < 0.664$ for on/off measurements of any symmetric detector efficiency higher than the threshold efficiency 67%. Similarly, the optimizing coherent amplitude for parity measurements is within the range $|\alpha| < 1.0$ when the detector efficiency is between the threshold (67%) and 97.7% [see Fig. 6(b)].

In real experiments, actual values of the detection efficiency for the two separate local measurements may be different. This realistic situation could be studied by taking the effective joint measurement defined by Eq. (11) with local detection efficiencies η_A and η_B. We plot the numerically optimized Bell function together with threshold regions for each measurement scheme in Fig. 7. The optimizing conditions have been found through nontrivial calculations as detailed in the Appendix. As presented in Fig. 8, the on/off measurement scheme provides higher violation of the Bell-CHSH inequality than the parity measurement scheme for most values of the detector efficiency.
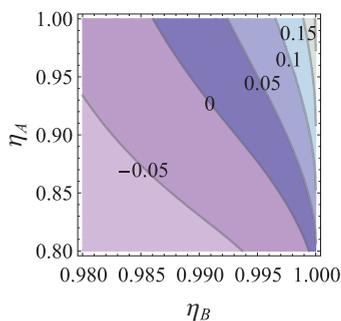
FIG. 8. (Color online) Subtracted value $|B|_{max}^{parity} - |B|_{max}^{on/off}$, values for different detection efficiencies η_A and η_B. Each $|B|_{max}$ is obtained by taking its optimizing coherent amplitude.

Only when the coherent field detection efficiency η_B is close to 1, parity measurements give higher Bell violation. Figure 7 shows that the conditions for the Bell-CHSH inequality to be violated are similar for two different measurement schemes. This can be attributed to the fact that the probability distributions for two different measurement schemes (i.e., "click" vs "no-click" for the on/off scheme and "odd" vs "even" or the parity one) are similar for low coherent amplitudes and low detection efficiency leads to the same optimizing conditions for both measurement schemes.

IV. REMARKS

We have studied a Bell inequality test with hybrid entanglement between polarization of a single photon and a coherent state field. We have investigated two different kinds of measurements, on/off and photon number parity measurement, on the coherent field to find Bell violations with optimizing conditions of perfect and realistic detectors. With perfect detectors, on/off measurements give the maximum Bell violation of ≈ 2.61 at $\alpha \approx 0.664$, while parity measurements give the violation approaching Cirel'son's bound ($2\sqrt{2}$) for large values of the coherent amplitude ($\alpha \gg 1$).

In order to see the Bell-CHSH inequality violation without the detection loophole, the detector efficiency $\eta > 67\%$ is required for both on/off and parity measurement schemes. It is important to note that small coherent amplitudes for hybrid entanglement are needed to obtain the low required efficiency, while there is a trade-off between the threshold efficiency and the degree of Bell violation in terms of the coherent amplitudes. Nevertheless, a coherent amplitude of $|\alpha| < 1.0$ is sufficient to obtain the maximum Bell violation for most cases of the detection efficiency. Comparing two different measurement schemes, we have found that on/off measurements provide higher violation of Bell inequality than parity measurements under realistic conditions ($\eta < 98.68\%$), although the violation does not reach Cirel'son's bound. However, the threshold values of detection efficiency to violate Bell inequality are similar between both measurement schemes.

Our results may be used to experimentally explore loophole-free Bell inequality tests. Required detection efficiency for a loophole-free Bell test is within reach of current technology [55–57]. The generation of hybrid entanglement is a challenging task since it requires a clean cross-Kerr nonlinearity, while efforts are being made to obtain high-fidelity cross-Kerr interactions [50–52]. It is also possible, in principle, to approximately generate arbitrary multimode entangled states using single-photon sources, coherent states, and single-photon detectors [58]. In this context, a possible attempt for the generation of hybrid entanglement is to explore combinations of experimentally available photon addition and subtraction techniques [59–64] as investigated for the generation of some exotic quantum states [65–67].

It is interesting to note that coherent states are considered most classical among all pure states, while single photons are typical microscopic quantum systems. In this sense, Bell inequality tests using the optical hybrid states may reveal a significant feature of nonlocality between quantum and classical systems. It will be an interesting future work to
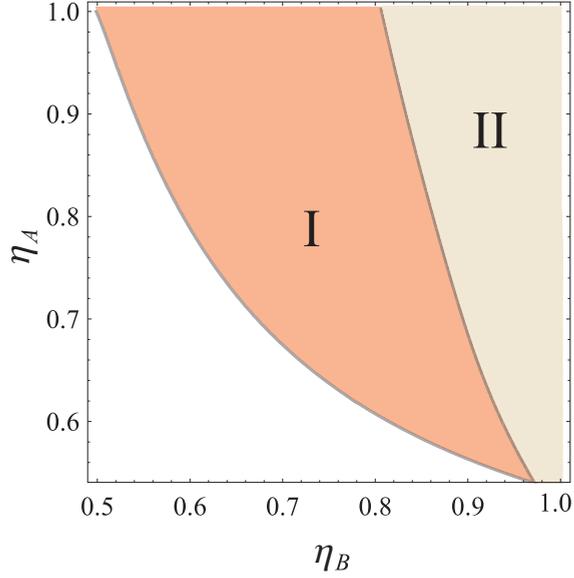
FIG. 9. (Color online) Optimizing conditions for parity measurements with detection efficiencies η_A and η_B. Shaded areas I and II are regions where the Bell-CHSH inequality is violated. Region I has optimizing conditions with real ξ and β, while region II has optimizing conditions with $|\xi| = \pi/4$ and pure imaginary β.

explore quantum nonlocality with optical hybrid entanglement using "classical" measurements [68,69].

APPENDIX: OPTIMIZING CONDITIONS FOR IMPERFECT DETECTOR EFFICIENCY

1. On/off measurements

We have numerically found maximum Bell values and corresponding optimizing conditions [54]. After numerical trials, we find that it is sufficient to take real values of the unitary parameters ξ and β in order to obtain those maximum Bell values for on/off measurements. Under this condition, Eqs. (13) and (14) can be represented in terms of θ and $|\beta|$ as

$$\langle \hat{O}_A \otimes \hat{O}_{B,\text{eff}}^{\text{on/off}} \rangle = \mp 2 \cos\theta e^{-\eta_B(|\alpha|^2+|\beta|^2)} \sinh(2\eta_B|\alpha||\beta|) - \sin\theta e^{-2|\alpha|^2} + 2\sin\theta e^{-(2-\eta_B)|\alpha|^2 - \eta_B|\beta|^2},$$

$$\text{Tr}_B\big[\hat{O}_{B,\text{eff}}^{\text{on/off}} \rho_B\big] = 2 e^{-\eta_B(|\alpha|^2+|\beta|^2)} \cosh(2\eta_B|\alpha||\beta|) - 1, \tag{A1}$$

where $\mp$ corresponds to negative or positive β. The Bell function B can be constructed using Eqs. (5) and (11). In order to find optimizing values, we take derivatives of B to be zero with respect to each parameter as

$$\left\{ \frac{\partial B}{\partial \theta_1}, \frac{\partial B}{\partial \theta_2}, \frac{\partial B}{\partial \beta_1}, \frac{\partial B}{\partial \beta_2} \right\} = 0, \tag{A2}$$

which leads to a set of equations

$$\tan\theta_1 = \frac{e^{-2(1-\eta_B)|\alpha|^2}(e^{-\eta_B|\alpha|^2} - e^{-\eta_B|\beta_1|^2} - e^{-\eta_B|\beta_2|^2})}{e^{-\eta_B|\beta_1|^2}\sinh(2\eta_B|\alpha||\beta_1|) - e^{-\eta_B|\beta_2|^2}\sinh(2\eta_B|\alpha||\beta_2|)},$$

$$\tan\theta_2 = -\frac{e^{-2(1-\eta_B)|\alpha|^2}(e^{-\eta_B|\beta_1|^2} - e^{-\eta_B|\beta_2|^2})}{e^{-\eta_B|\beta_1|^2}\sinh(2\eta_B|\alpha||\beta_1|) + e^{-\eta_B|\beta_2|^2}\sinh(2\eta_B|\alpha||\beta_2|)},$$

$$[|\beta_1|\sinh(2\eta_B|\alpha||\beta_1|) - |\alpha|\cosh(2\eta_B|\alpha||\beta_1|)](\cos\theta_1 - \cos\theta_2) - e^{-2(1-\eta_B)|\alpha|^2}|\beta_1|(\sin\theta_1 - \sin\theta_2) = 0,$$

$$\{[-|\beta_2|\sinh(2\eta_B|\alpha||\beta_2|) + |\alpha|\cosh(2\eta_B|\alpha||\beta_2|)](\cos\theta_1 + \cos\theta_2) - e^{-2(1-\eta_B)|\alpha|^2}|\beta_2|(\sin\theta_1 + \sin\theta_2)\}$$

$$+ \frac{2(1-\eta_A)}{\eta_A}[-|\beta_2|\cosh(2\eta_B|\alpha||\beta_2|) + |\alpha|\sinh(2\eta_B|\alpha||\beta_2|)] = 0. \tag{A3}$$

2. Parity measurements

The scheme based on parity measurements undergoes two different optimizing conditions subject to detection efficiencies η_A and η_B. Region I in Fig. 9 corresponds to optimizing conditions for low efficiency detectors, where real values of ξ and β are taken. We apply this condition to Eqs. (15) and (16) and obtain the expectation value as

$$E_{\text{eff}}^{\text{parity,low}} = \eta_A[\mp 2\cos\theta e^{-2\eta_B(|\alpha|^2+|\beta|^2)}\sinh(4\eta_B|\alpha||\beta|) + \sin\theta e^{-2(1-\eta_B)|\alpha|^2 - 2\eta_B|\beta|^2}]$$

$$+ (1-\eta_A)e^{-2\eta_B(|\alpha|^2+|\beta|^2)}\cosh(4\eta_B|\alpha||\beta|), \tag{A4}$$

where $\theta = -2\xi$ and $\mp$ corresponds to negative or positive β. Using Eq. (A2), we obtain a set of equations,

$$\tan\theta_1 = -\frac{e^{-2(1-2\eta_B)|\alpha|^2}(e^{-2\eta_B|\beta_1|^2} + e^{-2\eta_B|\beta_2|^2})}{e^{-2\eta_B|\beta_1|^2}\sinh(4\eta_B|\alpha||\beta_1|) - e^{-2\eta_B|\beta_2|^2}\sinh(4\eta_B|\alpha||\beta_2|)},$$

$$\tan\theta_1 = -\frac{e^{-2(1-2\eta_B)|\alpha|^2}(e^{-2\eta_B|\beta_1|^2} - e^{-2\eta_B|\beta_2|^2})}{e^{-2\eta_B|\beta_1|^2}\sinh(4\eta_B|\alpha||\beta_1|) + e^{-2\eta_B|\beta_2|^2}\sinh(4\eta_B|\alpha||\beta_2|)},$$

$$[|\beta_1|\sinh(4\eta_B|\alpha||\beta_1|) - |\alpha|\cosh(4\eta_B|\alpha||\beta_1|)](\cos\theta_1 - \cos\theta_2) - e^{-2(1-2\eta_B)|\alpha|^2}|\beta_1|(\sin\theta_1 - \sin\theta_2) = 0,$$

$$\{[-|\beta_2|\sinh(4\eta_B|\alpha||\beta_2|) + |\alpha|\cosh(4\eta_B|\alpha||\beta_2|)](\cos\theta_1 + \cos\theta_2) - e^{-2(1-2\eta_B)|\alpha|^2}|\beta_2|(\sin\theta_1 + \sin\theta_2)\}$$

$$+ \frac{2(1-\eta_A)}{\eta_A}[-|\beta_2|\cosh(4\eta_B|\alpha||\beta_2|) + |\alpha|\sinh(4\eta_B|\alpha||\beta_2|)] = 0, \tag{A5}$$

and find the optimizing conditions.

Optimization for the high detection efficiencies (region II in Fig. 9) can be obtained by taking $|\xi_1| = |\xi_2| = \pi/4$ and β as pure imaginary number. The expectation value then becomes

$$E_{\text{eff}}^{\text{parity,high}} = \eta_A e^{-2(1-\eta_B)|\alpha|^2 - 2\eta_B|\beta|^2}\cos(4\eta_B|\alpha||\beta| \pm \phi) + (1-\eta_A)e^{-2\eta_B(|\alpha|^2+|\beta|^2)}\cosh(4\eta_B|\alpha||\beta|), \tag{A6}$$

where ϕ is a phase factor of ξ and $\pm$ corresponds with negative or positive $-i\beta$. In this case, we take similar steps with Eq. (A2) but using a set of parameters $\{\phi_1, \phi_2, |\beta_1|, |\beta_2|\}$, and find optimizing conditions by solving a set of equations

$$e^{-2\eta_B|\beta_1|^2}\sin(4\eta_B|\alpha||\beta_1| + \phi_1) = e^{-2\eta_B|\beta_2|^2}\sin(4\eta_B|\alpha||\beta_2| - \phi_1),$$

$$e^{-2\eta_B|\beta_1|^2}\sin(4\eta_B|\alpha||\beta_1| + \phi_2) = -e^{-2\eta_B|\beta_2|^2}\sin(4\eta_B|\alpha||\beta_2| - \phi_2),$$

$$|\beta_1|[\cos(4\eta_B|\alpha||\beta_1| + \phi_1) - \cos(4\eta_B|\alpha||\beta_1| + \phi_2)] + |\alpha|[\sin(4\eta_B|\alpha||\beta_1| + \phi_1) - \sin(4\eta_B|\alpha||\beta_1| + \phi_2)] = 0,$$

$$|\beta_2|[\cos(4\eta_B|\alpha||\beta_2| - \phi_1) + \cos(4\eta_B|\alpha||\beta_2| - \phi_2)] + |\alpha|[\sin(4\eta_B|\alpha||\beta_2| - \phi_1) + \sin(4\eta_B|\alpha||\beta_2| - \phi_2)]$$

$$+ \frac{2(1-\eta_A)}{\eta_A}|\beta_2|e^{2(1-2\eta_B)|\alpha|^2} = 0. \tag{A7}$$

[1] A. Einstein, B. Podolsky, and N. Rosen, Phys. Rev. **47**, 777 (1935).

[2] J. S. Bell, Rev. Mod. Phys. **38**, 447 (1966).

[3] J. F. Clauser, M. A. Horne, A. Shimony, and R. A. Holt, Phys. Rev. Lett. **23**, 880 (1969).

[4] N. Gisin and A. Peres, Phys. Lett. A **162**, 15 (1992).

[5] D. Kaszlikowski, P. Gnaciński, M. Żukowski, W. Miklaszewski, and A. Zeilinger, Phys. Rev. Lett. **85**, 4418 (2000).

[6] T. Durt, D. Kaszlikowski, and M. Żukowski, Phys. Rev. A **64**, 024101 (2001).

[7] K. Banaszek and K. Wódkiewicz, Phys. Rev. Lett. **82**, 2009 (1999).

[8] H. Jeong, J. Lee, and M. S. Kim, Phys. Rev. A **61**, 052101 (2000).

[9] T. C. Ralph, W. J. Munro, and R. E. S. Polkinghorne, Phys. Rev. Lett. **85**, 2035 (2000).

[10] Z.-B. Chen, J.-W. Pan, G. Hou, and Y.-D. Zhang, Phys. Rev. Lett. **88**, 040406 (2002).

[11] K. Banaszek, A. Dragan, K. Wódkiewicz, and C. Radzewicz, Phys. Rev. A **66**, 043803 (2002).

[12] H. Jeong, W. Son, M. S. Kim, D. Ahn, and Č. Brukner, Phys. Rev. A **67**, 012106 (2003).

[13] M. A. Rowe, D. Kielpinski, V. Meyer, C. A. Sackett, W. M. Itano, C. Monroe, and D. J. Wineland, Nature (London) **409**, 791 (2001).

[14] M. Ansmann, H. Wang, R. C. Bialczak, M. Hofheinz, E. Lucero, M. Neeley, A. O'Connell, D. Sank, M. Weides, J. Wenner, A. N. Cleland, and J. M. Martinis, Nature (London) **461**, 504 (2009).

[15] J. S. Bell, J. Phys. C **2**, 41 (1981).

[16] E. Santos, Phys. Lett. A **200**, 1 (1995).

[17] S. J. Freedman and J. F. Clauser, Phys. Rev. Lett. **28**, 938 (1972).

[18] A. Aspect, P. Grangier, and G. Roger, Phys. Rev. Lett. **47**, 460 (1981).

[19] W. Tittel, J. Brendel, H. Zbinden, and N. Gisin, Phys. Rev. Lett. **81**, 3563 (1998).

[20] G. Weihs, T. Jennewein, C. Simon, H. Weinfurter, and A. Zeilinger, Phys. Rev. Lett. **81**, 5039 (1998).

[21] P. M. Pearle, Phys. Rev. D **2**, 1418 (1970).

[22] P. H. Eberhard, Phys. Rev. A **47**, R747 (1993).

[23] M. Giustina, A. Mech, S. Ramelow, B. Wittmann, J. Kofler, J. Beyer, A. Lita, B. Calkins, T. Gerrits, S. W. Nam, R. Ursin, and A. Zeilinger, Nature (London) **497**, 7448 (2013).

[24] S. Massar, S. Pironio, J. Roland, and B. Gisin, Phys. Rev. A **66**, 052112 (2002).

[25] M. Genovese, Phys. Rev. A **71**, 052314 (2005).

[26] D. Collins and N. Gisin, J. Phys. A **37**, 1775 (2004).

[27] N. Brunner, N. Gisin, V. Scarani, and C. Simon, Phys. Rev. Lett. **98**, 220403 (2007).

[28] T. Vértesi, S. Pironio, and N. Brunner, Phys. Rev. Lett. **104**, 060401 (2010).

[29] C. Vitelli, M. T. Cunha, N. Spagnolo, F. De Martini, and F. Sciarrino, Phys. Rev. A **85**, 012104 (2012).

[30] Y. Lim, M. Paternostro, M. Kang, J. Lee, and H. Jeong, Phys. Rev. A **85**, 062112 (2012).

[31] R. Chaves and J. B. Brask, Phys. Rev. A **84**, 062110 (2011).

[32] H. Nha and H. J. Carmichael, Phys. Rev. Lett. **93**, 020401 (2004).

[33] R. García-Patrón, J. Fiurášek, N. J. Cerf, J. Wenger, R. Tualle-Brouri, and P. Grangier, Phys. Rev. Lett. **93**, 130409 (2004).

[34] S.-W. Ji, J. Kim, H.-W. Lee, M. S. Zubairy, and H. Nha, Phys. Rev. Lett. **105** 170404 (2010).

[35] J. B. Brask, N. Brunner, D. Cavalcanti, and A. Leverrier, Phys. Rev. A **85**, 042116 (2012).

[36] N. Sangouard, J.-D. Bancal, N. Gisin, W. Rosenfeld, P. Sekatski, M. Weber, and H. Weinfurter, Phys. Rev. A **84**, 052122 (2011).

[37] N. Spagnolo, C. Vitelli, M. Paternostro, F. De Martini, and F. Sciarrino, Phys. Rev. A **84**, 032102 (2011).

[38] C. Simon and W. T. M. Irvine, Phys. Rev. Lett. **91**, 110405 (2003).

[39] J. Park, M. Saunders, Y.-i. Shin, K. An, and H. Jeong, Phys. Rev. A **85**, 022120 (2012).

[40] M. Araújo, M. T. Quintino, D. Cavalcanti, M. F. Santos, A. Cabello, and M. T. Cunha, Phys. Rev. A **86**, 030101(R) (2012).

[41] C. Teo, M. Araújo, M. T. Quintino, J. Minář, D. Cavalcanti, V. Scarani, M. T. Cunha, and M. F. Santos, Nat. Commun. **4**, 2104 (2013).

[42] D. L. Moehring, M. J. Madsen, B. B. Blinov, and C. Monroe, Phys. Rev. Lett. **93**, 090410 (2004).

[43] J. Volz, M. Weber, D. Schlenk, W. Rosenfeld, J. Vrana, K. Saucke, C. Kurtsiefer, and H. Weinfurter, Phys. Rev. Lett. **96**, 030404 (2006).

[44] D. N. Matsukevich, P. Maunz, D. L. Moehring, S. Olmschenk, and C. Monroe, Phys. Rev. Lett. **100**, 150404 (2008).

[45] S.-W. Lee and H. Jeong, Phys. Rev. A **87**, 022326 (2013).

[46] K. Park, S.-W. Lee, and H. Jeong, Phys. Rev. A **86**, 062301 (2012).

[47] H. Jeong, Phys. Rev. A **72**, 034305 (2005).

[48] J. H. Shapiro, Phys. Rev. A **73**, 062305 (2006).

[49] J. H. Shapiro and M. Razavi, New J. Phys. **9**, 16 (2007).

[50] B. He, Q. Lin, and C. Simon, Phys. Rev. A **83**, 053826 (2011).

[51] S. R. Mahdi Hosseini, B. M. Sparkes, J. Twamley, B. C. Buchler, and P. K. Lam, Light: Sci. Appl. **1**, e40 (2012).

[52] C. Chudzicki, I. L. Chuang, and J. H. Shapiro, Phys. Rev. A **87**, 042325 (2013).

[53] P. Kok and B. W. Lovett, *Introduction to Optical Quantum Information Processing* (Cambridge University Press, Cambridge, 2010).

[54] W. H. Press, B. P. Flannery, S.A. Teukolsky, and W. T. Vetterling, *Numerical Recipes* (Cambridge University Press, Cambridge, 1988).

[55] A. E. Lita, A. J. Miller, and S. W. Nam, Opt. Express **16**, 3032 (2008).

[56] R. H. Hadfield, Nat. Photonics **3**, 696 (2009).

[57] F. Marsili, V. Verma, J. Stern, S. Harrington, A. Lita, T. Gerrits, I. Vayshenker, B. Baek, M. Shaw, R. Mirin, and S. W. Nam, Nat. Photonics **7**, 210 (2013).

[58] J. Fiurášek, S. Massar, and N. J. Cerf, Phys. Rev. A **68**, 042325 (2003).

[59] A. Zavatta, S. Viciani, and M. Bellini, Science **306**, 660 (2004).

[60] J. Wenger, R. Tualle-Brouri, and P. Grangier, Phys. Rev. Lett. **92**, 153601 (2004).

[61] V. Parigi, A. Zavatta, M. S. Kim, and M. Bellini, Science **317**, 1890 (2007); R. W. Boyd, K. W. Chan, and M. N. O'sullivan, *ibid*. **317**, 1874 (2007).

[62] M. S. Kim, H. Jeong, A. Zavatta, V. Parigi, and M. Bellini, Phys. Rev. Lett. **101**, 260401 (2008).

[63] A. Zavatta, V. Parigi, M. S. Kim, H. Jeong, and M. Bellini, Phys. Rev. Lett. **103**, 140406 (2009).

[64] M. S. Kim, J. Phys. B **41**, 133001 (2008).

[65] P. Marek, H. Jeong, and M. S. Kim, Phys. Rev. A **78**, 063811 (2008).

[66] C.-W. Lee, J. Lee, H. Nha, and H. Jeong, Phys. Rev. A **85**, 063815 (2012).

[67] S.-Y. Lee, J. Park, H.-W. Lee, and H. Nha, Opt. Express **20**, 14221 (2012).

[68] H. Jeong, M. Paternostro, and T. C. Ralph, Phys. Rev. Lett. **102**, 060403 (2009).

[69] P. Sekatski, N. Brunner, C. Branciard, N. Gisin, and C. Simon, Phys. Rev. Lett. **103**, 113601 (2009).